A comparative study of zwitterionic ligands-mediated mineralization and the potential of mineralized zwitterionic matrices for bone tissue engineering

Pingsheng Liu, **Erin Emmons**, and **Jie Song**

Department of Orthopedics & Physical Rehabilitation, Department of Cell and Developmental Biology, University of Massachusetts Medical School, Worcester, MA 01655, USA

Jie Song: Jie.song@umassmed.edu

Abstract

Cationic and anionic residues of the extracellular matrices (ECM) of bone play synergistic roles in recruiting precursor ions and templating the nucleation, growth and crystalline transformations of calcium apatite in natural biomineralization. We previously reported that zwitterionic sulfobetaine ligands can template extensive 3-dimensional (3-D) hydroxyapaptite (HA)-mineralization of photo-crosslinked polymethacrylatehydrogels. Here, we compared the potency of two other major zwitterionic ligands, phosphobetaine and carboxybetaine, with that of the sulfobetaine in mediating 3-D mineralization using the crosslinked polymethacrylate hydrogel platform. We confirmed that all three zwitterionic hydrogels were able to effectively template 3-D mineralization, supporting the general ability of zwitterions to mediate templated mineralization. Among them, however, sulfobetaine and phosphobetaine hydrogels templated denser 3-D mineralizationthan the carboxybetaine hydrogel, likely due to their higher free water fractions and better maintenance of zwitterionic nature throughout the pH-changes during the *in vitro* mineralization process. We further demonstrated that the extensively mineralized zwitterionic hydrogels could be exploited for efficient retention (e.g. 99% retention after 24-h incubation in PBS) of osteogenic growth factor recombinant bone morphogenetic protein-2 (rhBMP-2) and subsequent sustained local release with retained bioactivity. Combined with the excellent cytocompatibility of all three zwitterionic hydrogels and the significantly improved cell adhesive properties of their mineralized matrices, these materials could find promising applications in bone tissue engineering.

Introduction

Natural biomineralization of calcified tissue is a complex process involving cellular activities and extracellular matrices (ECM)-mediated ion transport, heterogeneous nucleation, and oriented mineral growth and crystalline phase transitions[1–4]. In this process, both acidic non-collagenous proteins (NCPs) and collagen fibrils are believed to play important roles in facilitating precursor ion/calcium phosphate clusters infiltration,

Correspondence to: Jie Song, Jie.song@umassmed.edu.

stabilizing initial amorphous calcium phosphate deposition (ACP), and templating/modulating subsequent transformation of ACP into more stable crystalline hydroxyapatite (HA) phase[2, 3, 5–15]. Acidic NCPs (e. g. phosphoproteins) have long been identified as the pre-nucleation cites for calcium phosphate (CaP) and as the mediator of the subsequent transformation of ACP into oriented apatite crystals[4–6, 16]. A more recent study on the role of collagen in templating mineralization in the presence of HA nucleation inhibitors suggests that the positive net charge close to the C-terminus of the collagen molecules promotes the infiltration of ACP into the collagen fibrils while the negatively charged amino acids, both in gap and overlapping regions of collagen fibrils, form nucleation sites mediating the transformation of ACP into oriented apatite crystals[17]. These findings suggest that the oppositely charged residues in the ECM synergistically facilitated the natural biomineralization.

Inspired by nature, we recently reported the strategic utilization of zwitterionic sulfobetaine ligand, possessing equal number of oppositely charged residues yet overall electrically neutral, for templating extensive 3D HA-mineralization of synthetic hydrogel scaffolds[18]. Compared with the cationic matrices, the zwitterionic sulfobetaine matrix exhibited better cyto-compatibility[19–26] and also enabled more extensive 3D mineralization throughout the hydrogel matrix than both cationic and anionic matrices[18]. We hypothesize that the ability of the sulfobetaine to effectively recruit oppositely charged precursor ions and to mediate the templated-mineralization is generalizable to zwitterion family in general.

HA and related calcium phosphate minerals have been intensively investigated for orthopedic applications[27, 28] due to their biocompatibility and the ability to support the attachment and proliferation bone cells (osteoconductivity)[28, 29] and promote osteochondral lineage commitment of bone marrow-derived stromal cells[30]. The large surface area and surface charge of HA can also be exploited for loading and sustained local delivery of osteoinductive growth factors (e. g. BMPs) to facilitate the osseointegration[31–35]. Thus, extensively mineralized zwitterionic matrices with well-integrated organic-inorganic interfaces throughout the scaffolds[18] are rational candidates as osteoconductive tissue scaffolds as well as delivery vehicles for osteoinductive protein factors for skeletal tissue regeneration. To the best of our knowledge, the utilization of mineralized zwitterionic matrices for delivery of osteoinductive growth factor has never been reported.

Accordingly, in the current study, we first compared the potency of three types of zwitterionic ligands, sulfobetaine, phosphobetaine and carboxybetaine, covalently presented in photo-crosslinked polymethacrylate hydrogel networks with identical crosslinker content, in templating 3D mineralization of calcium apatite. The mineral volume, mineral density and total Ca^{2+} content of the three mineralized zwitterionic composites were quantitatively compared. The swelling ratio, free water fractions of the zwitterionic hydrogels and the ionic state of the respective zwitterionic polymers during the mineralization were investigated to elucidate factors underlying the differential mineralization outcomes observed. We then evaluated cell adhesive properties and rhBMP-2 retention/release profiles of the un-mineralized *vs* mineralized polysulfobetaine methacrylate (PSBMA) hydrogels to elucidate the potential of mineralized zwitterionic matrices for osteogenic protein delivery and bone tissue engineering applications.

Experimental

Preparation of hydrogels

Methacryloyloxyethyl phosphorylcholine) (PMPC), poly[3-((2-(methacryloyloxy)ethyl)dimethylammonio)propanoate] (PCBMA) and poly(ethylene glycol) methacrylate (PEGMA) were photo-crosslinked from monomers SBMA (Aldrich), MPC (Aldrich), CBMA (synthesized according to literature[36]) and PEGMA (M_n = 360, Aldrich) in the presence of crosslinker poly (ethylene glycol) dimethacrylate (PEGDMA, M_n = 750). The radical inhibitors in PEGMA and PEGDMA were removed by passing through an aluminum oxide column prior to use. In a typical procedure, 2 mmol of the respective monomer was combined with 17.9 μL of PEGDMA, 100 μL of PBS solution of 2,2'-Azobis[2-methyl-N-(2-hydroxyethyl)propionamide] (VA-086, 2 %, w/v, Wako), and 1882.1 μL of PBS. The mixture was bath-sonicated, and sterilized by passing through a 0.22-μm polyethersulfone (PES) membrane filter (Millipore). The resulting solution was transferred to a custom-made Teflon mold with cylindrical (6 mm in diameter, 50 μL/well) or cubic (5 mm × 5mm, 50 μL/well) wells and solidified under the irradiation of 365-nm light for 10 min in a sterile hood. The hydrogels were stored in sterile PBS until further uses.

Swelling ratio measurement of the hydrogels

The swelling ratios of the hydrogel by weight (S_w) were determined in PBS (pH=7.4) at room temperature according to Equations 1:

$$S_w = \frac{W_h - W_d}{W_h} \quad \text{Eq-1}$$

where W_h and W_d are the weight of a hydrogel in fully hydrated state and dry state, respectively.

Mineralization of the hydrogels

Mineralization was carried out by controlled heating of the hydrogels in a urea-containing, acidic aqueous solution of hydroxyapatite from 37 °C to 95 °C using a protocol modified over a previous report[37]. Mineralization stock solution was prepared by suspending hydroxyapatite (7.37 g, 34–40% Calcium content, Alfa Aesar) in 500-mL aqueous solution of urea (2 M), followed by the addition of concentrated hydrochloric acid under constant stirring until a clear soluble solution was obtained (final pH 2.5–3.0). Six to ten hydrogels were placed in an Erlenmeyer flask filled with 30 mL of mineralization solution and covered with a perforated aluminum foil. The flask was placed in a high-temperature silicone oil bath with the mineralization solution completely submerged under the oil and heated using a 100-watt immersion heater (Glo-Quartz LHP-IAH4) equipped with a programmable temperature controller (Eurotherm 2408). Controlled heating from 37 °C to 95 °C was carried out at a heating rate of 0.2 °C/min. Mineralized hydrogels were bath-sonicated for 1 min in Milli-Q water to ensure removal of loosely bound minerals, followed by further incubation in fresh Milli-Q water at 37 °C for two days with regular water change once every 12 h to ensure removal of the residual mineralization precursor ions trapped within the mineralized hydrogel prior to quantification of the content of tightly bound minerals.

Microcomputed tomography (μ-CT)

Mineralized hydrogel specimens (N = 3) were scanned on a Scanco μCT40 scanner. The effective voxel size of the reconstructed images was $8 \times 8 \times 8$ μm^3. Data were globally thresholded and reconstructed to quantify the mineral volume (MV, mm^3) and mineralization density (mineral volume/hydrogel volume, MV/HV) of the composites as determined by a direct analysis model. An unmineralized hydrogel was also scanned as a negative control to ensure proper setting of the threshold for analyses.

Quantification of total Ca2+-content of the mineralized hydrogels

Total calcium content was determined by quantifying the Ca^{2+} ions released from each mineralized hydrogel in a hydrochloric acid solution with a Thermo Scientific calcium ion selective electrode attached to a VWR Symphony pH/ISE meter. In a typical procedure, the mineralized hydrogel was placed in 10 mL of hydrochloric acid solution (pH 3) in a 20 mL glass vial and the pH was adjusted by concentrated hydrochloric acid to around 2.1. The mineral was allowed to be fully released from the hydrogel under constant shaking of the acidic solution on an orbital shaker, as indicated by reaching a transparent appearance of the gel. Ionic Strength Adjustment buffer (ISA, 4 M KCl solution, VWR, 200 μL) was added to the acidic solution containing the released calcium prior to measurement by the calcium ion selective electrode. The total calcium content of each type of mineralized hydrogel (N = 3) was determined using a standard curve generated by a series of acidic (pH 2.1) aqueous Ca^{2+} ion standard solutions containing 0.1, 0.01, 0.001, and 0.0001 M $CaCl_2$.

Water fraction measurement of the zwitterionic hydrogels

The free water fraction in the hydrogels was measured by differential scanning calorimetry (DSC) on a Q200 Modulated DSC (TA Instruments).About 15 mg of hydrogel equilibrated in PBS was placed in an aluminum pan. The pan was then sealed tightly to prevent water evaporation during the measurement. The testing was carried out from −40 °C to 40 °C at a heating rate of 2 °C/min. The exothermal peak around 0°C, attributed to the melting of the free water[38], was calculated as H_{endo}, and the free water fraction (R_f) within the hydrogel was determined according equation 2:

$$R_f = \frac{\Delta H_{endo}}{\Delta H_w} \quad \text{Eq-2}$$

where H_w is the heat fusion of pure water (332.2 mJ/mg)[19].

Scanning electron microscopy (SEM) and associated Energy dispersive X-ray spectroscopy (EDS)

The morphologies at both the surface and the cross-section of airdried mineralized hydrogels, sputter coated with 4-nm gold, were observed by SEM on a Quanta 200 FEG MKII microscope equipped with an Oxford-Link Inca 350 X-ray spectrometer (Oxford Instruments) under an accelerating voltage of 10 kV and a spot size of 3.0 μm. For the cross-section observation, air-dried or freezedried mineralized hydrogels were bisected by a razor blade. EDS spectra and calcium and phosphorus elemental mapping were acquired for 2 min under the same conditions (except for aperture size). Reported calcium to phosphorus ratios

(Ca:P) were based on calibration using single crystal HA whiskers prepared by molten salt synthesis (Ca:P = 1.67)[39].

Preparation of linear zwitterionic polymers

To measure the ionic state of the zwitterionic matrices during the gradual pH increases of the mineralization process, zwitterionic linear polymers were prepared through the atom transfer radical polymerization according to the protocol previously reported.[40] In a typical procedure, BPY (0.2 mmol) was dissolved in TFE in a Schlenk flask and degassed by three "freeze-pump-thaw" cycles to remove oxygen. The flask was then back-filled with argon and CuBr (0.1 mmol) was added into the flask under the argon protection. The mixture was stirred for 10 min to ensure the formation of the copper catalyst complex. Monomer (5 mmol, for DP = 50), free initiator EBiB (0.1 mmol), and HMImCl (10 wt% to TFE) were dissolved in TFE under stirring in the second Schlenk flask at room temperature. The flask was then degassed by three "freeze-pump-thaw" cycles, after which the copper catalyst complex was added by syringe. The mixture was allowed to stir for an additional 1 min before the flask was mounted in an isothermal water bath to start the polymerization. After the completion of the reaction, the mixture was exposed to air and then desalted in a dialysis membrane tubing (Spectra/Por 6, MWCO: 1000) against Milli-Q water for 72 h, with regular change of fresh Milli-Q water every 8 h. The resulting desalted solutions were then freeze-dried to obtain the linear zwitterionic polymers as white powders.

Aqueous gel permeation chromatography (GPC)

The molecular weight and molecular weight distribution measurement of the zwitterionic polymers were performed on a Varian ProStar HPLC system connected with two PL Aquagel-OH columns (type 40 first, followed by type 20, 8 mm, 300×7.5mm, Agilent Technologies) and equipped with a refractive index detector (Varian 356-LC, 35 °C). The eluent was 0.05 M Trisma buffer (pH 7.0) containing 0.2 M $NaNO_3$ and a flow rate of 1.0 mL/min was applied. Weight- and number-averaged molecular weights (M_w and M_n) and polydispersity index (PDI) of the polymers were calculated by Cirrus AIA GPC software. Ten narrowly dispersed PEO standards from PL2070-0100 and PL-2080-0101 kits (Polymer Laboratories, Agilent Technologies) were used as calibration standards.

Zeta potential of zwitterionic matrices

To examine the ionic state of the zwitterionic ligands as a function of pH changes during the mineralization, the zeta potentials of linear PSBMA polymer under pH ranging from 3 to 9 were measured on a Zetasizer (Zen3600, 633 nm laser, Malvern). Linear pSBMA solutions (3 mg/mL in 0.015 M NaCl aq. solution) were adjusted to achieve targeted pH by aqueous HCl or NaOH, and placed in disposable capillary cells (DTS1061, Malvern) for zeta potential measurement at 25 °C.

Cell encapsulation in hydrogels

The cyto-compatibility of three types of zwitterionic hydrogels, PSBMA, PMPC, and PCBMA, were investigated by the viability of rat bone marrow stromal cells (rMSCs) encapsulated in these hydrogels. In a typical procedure, 2 mmol of the respective monomer

was dissolved in 2 mL of expansion medium (α-MEM supplemented with 20% FBS, 1% penicillin, 1% streptomycin, and 2% glutamine) mixed with 100 μL of 2 wt% VA-086 PBS solution and a pre-determined amount of water-soluble crosslinker polyethylene glycol dimethacrylate (PEGDMA, M_n = 750). The mixture was sterile-filtered through a 0.2 μm sterile polyethersulfone syringe filter. Passage 1 rMSC, isolated from the femoral marrow canal of skeletally mature SASCO SD rats (Charles River Lab, 8–10 week old) and enriched by adherent culture[18], were plated in expansion medium for 24 h before they were trypsinized, counted, and suspended into the respective monomer/crosslinker/initiator mixtures (10^6 cells/mL). The rMSC-containing solution was then transferred to a custom-made Teflon mold of square prism wells (5 mm × 5 mm; 50 μL/well) and solidified under the irradiation of 365-nm light for 10 min in a sterile hood. All cell–hydrogel constructs were cultured for up to 7 days in humidified incubation (5% CO_2, 37 °C) before being subjected to live/dead cell staining. Cyto-compatible PEGMA hydrogels prepared by crosslinking PEGMA monomer (M_n = 360) with the identical crosslinker content of 1.33 mol% relative to monomer served as a control.

Live/dead cell staining and confocal microscopy

The hydrogel–cell constructs were stained using a LIVE/DEAD viability/cytotoxicity kit (Molecular Probes) following the vendor's protocol. Live cells were stained with green fluorescence by intracellular esterase-catalyzed hydrolysis of Calcein AM, and dead cells were stained red by ethidium homodimer-1 penetrated through the damaged membranes and bound with nucleic acids. After being stained for 30–45 min at 37 °C, the stained hydrogel–cell construct was retrieved and mounted in a Cellview culture dish (Greiner) and imaged on a Leica TCS SP2 confocal microscope. Calcein was excited at 488 nm and observed with the FITC filter (518–542 nm) while ethidium homodimer-1 was excited at 543 nm and observed with the TEXAS RED filter (625–665 nm). Confocal Z-stack images of encapsulated rMSC over the depth of 80 μm (8 consecutive 10 μm slices) were overlaid.

In vitro release of rhBMP-2 from mineralized vs unmineralized PSBMA hydrogels

Recombinant protein rhBMP-2 (R&D Systems, CHO-derived) was reconstituted according to vendor specifications and diluted with Ca^{2+}/Mg^{2+}-free Dulbecco's phosphate-buffered saline (DPBS, pH 7.4) to a loading concentration of 30 ng/μL. Hydrogels retrieved from the sterile stock solution were partially dried in a sterile cell culture hood (with a total gel volume reduction of 50 to 100 mm^3), and then transferred into the wells of ultra-low attachment 24-well plate (Corning). Reconstituted rhBMP-2 solution (10 μL, 30 ng/ μL) was placed on each hydrogel (cylindrical specimens) to achieve a total loading dose of 300-ng rhBMP-2/hydrogel, and allowed to be incubated at 37 °C for 1 h to ensure full absorption of the rhBMP-2 solution by the hydrogels. The rhBMP-2 loaded hydrogels were then incubated in 1 mL of DPBS at 37 °C for 2, 4, 6, 10, and 24 h. Concentrations of the rhBMP-2 released into the DPBS at various time points were determined by an enzyme-linked immuno sorbent assay (ELISA) using rhBMP-2 Quantikine Kits, (R&D Systems) and the amount of the rhBMP-2 released form hydrogels were calculated from the standard curve generated during the same experiment. A sample size of 3 was applied to each hydrogel group.

Sustained release of bioactive rhBMP-2 from the mineralized PSBMA hydrogels

The bioactivity of the rhBMP-2 retained on and subsequently released from the mineralized PSBMA hydrogels was evaluated by their ability to induce osteogenic trans-differentiation of murine myoblast C2C12 cells into osteoblasts[34, 41]. C2C12 cells were seeded on 24-well cell culture plate (10,000 cells/cm^2) in 1 mL of Dulbecco's modified eagle medium (DMEM) supplemented with 10% fetal bovine serum and 1% penicillin/streptomycin, and allowed to attach overnight. The medium was then replaced with fresh DMEM supplemented with 5% fetal bovine serum and 1% penicillin/streptomycin, and the rhBMP-2 loaded hydrogels retrieved from prior incubation in PBS up to 6 days were placed in the adherent C2C12 culture. After 3 days, the hydrogel was removed and the cells were fixed and stained for alkaline phosphatase (ALP) using a Sigma Leukocyte Alkaline Phosphatase Kit according to the vender's protocol. C2C12 culture directly supplemented with 300-ng rhBMP-2 without any hydrogel carrier served as a positive control.

Cell attachment to the mineralized and un-mineralized PSBMA hydrogels

The cell attachment onto the zwitterionic PSBMA hydrogel and mineralized PSBMA hydrogel were measured by the CCK-8 cell viability kit. rMSC were suspended in fresh MSC expansion medium at a density of 50,000 cell/ml. Cylinder hydrogel specimens, retrieved from the sterile stock solution and pre-equilibrated in expansion medium, were transferred into a sterile ultra-low attachment 24-well plate (Corning) followed by the addition of 1 mL fresh cell suspension into each well. After being cultured for 24 h in a humidified incubator (5% CO$_2$, 37 °C), the hydrogels were retrieved, gently rinsed with sterile culture medium to remove unattached cells, and placed in another sterile ultra-low attachment 24-well plate with the addition of 0.6 mL fresh cell culture medium and 60 μL of CCK-8 reagent. The cell-hydrogel construct were cultured for 4 h in the humidified incubator (5% CO$_2$, 37 °C). The absorbance of the collected supernatant (100 μL, N=3) was read at 450 nm (with background correction read at 620 nm) on a MULTISCANFC spectrophotometer (Thermo Scientific). Non-ionic anti-fouling PEGMA hydrogel with identicalcrosslinker content to that in zwitterionic PSBMA hydrogel (1.33 mol% relative to monomer) served as a control.

Results and discussion

To test the hypothesis that the ability to mediate templated-mineralization is general to the zwitterion family, three types of representative zwitterionic ligands (sulfobetaine, phosphobetaine and carboxybetaine) were covalently incorporated in polymethacrylate hydrogel networks by photo-crosslinking the methacrylate monomer bearing respective zwitterionic motifs with an identical crosslinker content (1.33 mol% relative to monomer, Fig. 1a). The photo-crosslinked polymethacrylate hydrogels were placed in the mineralization solution and subjected to heterogeneous HA-mineralization driven by gradual pH increases resulting from controlled thermal decomposition of urea upon heating from 37 °C to 95 °C at a rate of 0.2 °C/min[37, 42]. As expected, all three hydrogels were substentially mineralized, with their physical appearances chaging from transparent gels to opaque white composites (Figs. 1b, c) and spherical mineral domains formed across the 3D hydrogels (Fig. 1d). Reconstructed μ-CT cross-sectional views of these mineralized zwitterionic

hydrogels confirmed extensive 3D mineralization (Fig. 2a). Using a combinbation of focused-ion beam (FIB) processing, high-resolution TEM and associated selected area electron diffraction (SAED), we previously confirmed that the mineral templated by PSBMA hydrogels were highly crystalline HA[18]. In the current study, we compared the Ca/P ratios of the apatite cyrstals formed within the three zwitterionic hydrogels by SEM associated EDS (Figs. 2b & c), and showed that they were close to (e.g. ~1.5) that of the theoretical Ca/P ratio for HA (1.67) without statistically significant difference among the three groups. Combined with the similar mineral densities (no significant difference) among the three mineralized composites as revealed by μ-CT analyses (Fig. 2d), these data support that zwitterions are generally effective in recruiting mineralization precursor ions and in templating 3D mineralization.

The extent of templated mineralization, however, varied among the three different zwitterionic hydrogels. Upon acid treatment, PMPC hydrogels released the highest Ca^{2+} content (41 μmol Ca^{2+} per hydrogel), almost twice and 5 times of those detected from mineralized PSBMA and PCBMA hydrogels, respectively (Fig. 3a). Slimilar trend was observed with the mineral volume of the respective composites as determined by μ-CT analysis (Fig. 3b). Meanwhile, the volume fraction of mineralized matrices (mineral volume devided by the hydrogel volume, MV/HV) within the PSBMA and PMPC composites were nearly identical, both doubling that of the PCBMA composite (Fig. 3c). Overall, these data indicate that sulfobetaine and phosphobetaine are more effective mediators than carboxybetaine for the templated 3D mineralization.

Crosslinking densities, swelling ratios and free water fractions of hydrogels,[38] along with their chemical nature, can all affect the diffusibility of solutes/precursor ions across the 3-D matrices[38]. Given the identical crosslinking degree applied to all three zwitterionic hydrogels (1.33 mol% relative to monomers), we first investigated whether the differential swelling ratios or free water fractions of these hydrogels may have contributed to the different mineralization outcomes observed. We found that the phosphobetaine (PMPC) and carboxybetaine (PCBMA) hydrogels swelled almost twice as much as that of the sulfobetaine hydrogel (PSBMA) in PBS (Fig. 4a), which did not correlate with their relative degrees of mineralization (Fig. 3). In fully equilibrated hydrogels, water are either structurally bound to the polymer matrices or present as "free" water functioning as the medium for solute transport[38]. We showed that the free water fractions (Fig. 4b) in the PSBMA and PMPC were nearly identical, but slightly higher than that in the PCBMA (statistically significant). This trend in free water fractions is consistent with that of the degree of mineralization templated by these hydrogels, suggesting that free water fractions may have played a more significant role than the overall swelling ratio in enabling more effective infiltration of the precursor ions across the hydrogel matrices.

We then examined whether and how the differences in chemical structures of the zwitterionic motifs contributed to the varied degrees of mineralization. The *in vitro* mineralization process utilized in this study was modulated by the thermal decomposition of the urea present in the mineralization solution, which resulted in gradual increases of the solution pH driving super-saturation[37]. Specifically, the pH of this mineralization process increased from 2.6 to 7 at the given heating rate of 0.2 °C/min.[18] Faced with the difficulty in

directly measuring the ionic state of the zwitterionic motifs presented in 3D crosslinked hydrogel networks, we prepared linear zwitterionic polymers by atom transfer radical polymerization (Table 1) and measured their zeta potentials as a function of pH changes. As showed in Figure 5a, at the onset of the mineralization process (pH < 3), the linear carboxybetaine polymer exhibited an overall positive charge (~ +4 mV) while the sulfobetaine and phosphobetaine polymers were almost electric neutral, thereby maintaining their zwitterionic nature. This trend persisted up till pH of 4.11, constituting nearly 80% of the mineralization duration (Fig. 5b), before the zwitterionic carboxybetaine polymer reached the electric neutral state. Given that all three zwitterionic motifs consist of the same cationic quaternary ammonium residue, their different anionic residues are likely responsible for their difference in pH-dependent ionic state. The carboxyl group has a logarithmicacid dissociation constants (pK_a) of 4.76[43], which is higher than that of the sulfonate group (pK_a = 1)[44] or the phosphate group (pK_a = 1.39)[45], meaning that the carboxylates are far more prone to protonation. This suggests that the zwitterionic nature of carboxybetaine is more likely be compromised at lower pH, consistent with the zeta potential data. The ability of sulfobetaine and phosphobetaine ligands to better maintain their zwitterionic nature than carboxybetaine during mineralization process may have translated into more sustained synergistic recruitment of oppositely charged precursor ions and ultimately more extensive mineralization.

To evaluate the potential of these zwitterionic hydrogels for bone tissue engineering applications, their cytocompatibility were examined by the viability of bone marrow stromal cells (rMSCs) encapsulated within these hydrogels. The cell-hydrogel constructs were cultured up to 7 days before subjected to live/dead staining to visualize the cell viability. Figure 6 showed that the MSCs encapsulated in all zwitterionic hydrogels remained viable by day 7, comparable to those encapsulated in the benchmark cytocompatible PEGMA hydrogels. This observation is consistent with the well-established biocompatibility of zwitterionic materials[19–26].

We recently showed that zwitterionic ligands, when 3D presented in hydrogel matrix, can retain and enable high-efficiency local delivery of ionic osteogenic recombinant human bone morphogenetic protein-2 (rhBMP-2) and template the functional healing of critical long bone defects in rats with an exceptionally low dose of rhBMP-2 (500 ng/scaffold)[46]. This was accomplished by virtue of the dynamically interaction between the 3D presented zwitterionic motifs and the ionic proteins. Here we examined whe ther the mineralized zwitterionic scaffolds may present further advantage in growth factor delivery. Specifically, we compared the *in vitro* retention/release of rhBMP-2 from mineralized *vs* unmineralized PSBMA hydrogels. We loaded 300 ng of rhBMP-2 solution to each partially dried PSBMA or mineralized specimen and allowed the solution to be fully absorbed at 37 °C for 1 h before the specimens were subjected to incubation in PBS for the *in vitro* release study. We showed that the unmineralized PSBMA retained ~68% of the rhBMP-2 after 2-h incubation in PBS (Fig. 6a), followed by an additional 3% of slow release in the next 22 h (Fig. 6b). Upon mineralization, the PSBMA-HA composite exhibited markedly improved retention of rhBMP-2, with ~99% retained after 2 h incubation and only 0.3 % of additional rhBMP-2 was released in the next 22 h (Fig. 7a, b). This finding suggests that the large surface areas

of the calcium apatite mineral components (Fig. 7c) and the electrostatic interaction of the mineral surface lattice with the ionic protein factor [47, 48] enabled the stable absorption of the protein. This observation is also consistent with literature findings of the role of calcium phosphate minerals (e. g. HA, TCP) in improving the efficiency of delivery of BMPs[47–51].

Equally important, we showed that the rhBMP-2 retained by the mineralized PSBMA hydrogel after 6-day incubation in PBS remained bioactive, as supported by the ability of the subsequently released rhBMP-2 to induce osteogenic trans-differentiation of murine myoblast C2C12 cells, an established *in vitro* culture model for assessing the osteoinductivity of rhBMP-2[34, 41]. This model was chosen over BMP-2-induced osteogenesis of mesenchymal stem cells (MSCs) due to the complete lack of expression of osteogneic markers by C2C12 cells prior to BMP-2 induction (thus much cleaner background than MSCs). Robust osteogenic trans-differentiation of C2C12 cells into alkaline phosphatase (ALP)-expressing osteoblasts (Fig. 7d) as indicated by intense ALP staining, slightly stronger than that of the positive control culture where 300-ng rhBMP-2 was directly supplemented without any carrier, suggest that the mineralized PSBMA hydrogel is an promising vehicle for sustained local delivery of rhBMP-2 with protected bioactivity. We recently reported the functional healing of 5-mm rat femoral segmental defects enabled by PSBMA hydrogel implants bearing an exceptionally low dose of 500-ng rhBMP-2. Here we expect that the better retention of rhBMP-2 by the mineralized zwitterionic PSBMA may translate into further improved scaffold/growth factor-enabled bone healing, potentially with an even lower loading dose of rhBMP-2.

Finally, we compared the cell-adhesive properties of the mineralized PSBMA surface *vs* that of the PSBMA, which is known for low-fouling properties comparable to that of the benchmark anti-fouling material PEGMA[19, 20, 23–26]. We showed that whereas limited MSCs adhered onto the surface of the zwitterionic PSBMA, comparable to that observed with the PEGMA hydrogels (Fig. 8) and consistent with literatures[52–56], the mineralized PSBMA composites supported much better surface attachment of MSCs (~100% increase). This observation supports that the osteoconductive surface mineral[28, 29] effectively overcame the low cell adhesive properties of the zwitterionic hydrogel, which is beneficial to the desired recruitment and adhesion of endogenous stem/progenitor cells and scaffold/ tissue integration *in vivo*.

Conclusion

In this study, we first compared the potency of three representative zwitterionic ligands, sufobetaine, phosphobetaine and carboxybetaine, in templating 3D mineralization of photo-crosslinked polymethacrylate hydrogels. All zwitterionic hydrogels were mineralized with spherical apatite mineral domains throughout the 3D networks, supporting the general ability of zwitterions to mediate templated mineralization. However, sulfobetaine and phosphobetaine hydrogels supported more extensive mineralization than the carboxybetaine hydrogel. The higher free water fractions in the sulfobetaine and phosphobetaine network, enabling better diffusion of the mineralization precursor ions, and their better maintained zwitterionic nature during the mineralization process, permitting more sustained recruitment of oppositely charged precursor ions, are likely responsible for the better templated

mineralization outcome. We then showed that the mineralization of the zwitterionic matrices also improved surface cell attachment due to the osteoconductivity of the calcium phosphate apatite, overcoming the intrinsic low cell adhesive properties of the otherwise low-fouling zwitterionic hydrogel. Furthermore, the mineralized zwitterionic matrices also enabled outstanding retention and local delivery of rhBMP-2 without compromising the bioactivity of the growth factor. Taken together, these findings support zwitterionic ligands as promising modalities to be integrated in the design of biomineralization templates in general. They can be implemented in the design of degradable bone tissue engineering scaffolds, and the mineralized zwitterionic composites may be exploited as more effective delivery vehicles of osteogenic protein therapeutics.

Acknowledgements

Notes and references

1. Mann S. Nature. 1988; 332:119–124.

2. Weiner S, Wagner HD. Annu. Rev. Mater. Sci. 1998; 28:271–298.

3. Traub W, Arad T, Weiner S. Proc. Natl. Acad. Sci. U. S. A. 1989; 86:9822–9826. [PubMed: 2602376]

4. George A, Veis A. Chem. Rev. 2008; 108:4670–4693. [PubMed: 18831570]

5. Hunter GK, Goldberg HA. Biochem. J. 1994; 302:175–179. [PubMed: 7915111]

6. Tye CE, Rattray KR, Warner KJ, Gordon JAR, Sodek J, Hunter GK, Goldberg HA. J. Biol. Chem. 2003; 278:7949–7955. [PubMed: 12493752]

7. He G, Dahl T, Veis A, George A. Nat. Mater. 2003; 2:552–558. [PubMed: 12872163]

8. Veis A, Perry A. Biochemistry-Us. 1967; 6:2409–2416.

9. George A, Bannon L, Sabsay B, Dillon JW, Malone J, Veis A, Jenkins NA, Gilbert DJ, Copeland NG. J. Biol. Chem. 1996; 271:32869–32873. [PubMed: 8955126]

10. Olszta MJ, Cheng XG, Jee SS, Kumar R, Kim YY, Kaufman MJ, Douglas EP, Gower LB. Mat. Sci. Eng. R. 2007; 58:77–116.

11. Jahnen-Dechent W, Heiss A, Schäfer C, Ketteler M. Circ. Res. 2011; 108:1494–1509. [PubMed: 21659653]

12. Boskey AL, Spevak L, Paschalis E, Doty SB, McKee MD. Calcified Tissue Int. 2002; 71:145–154.

13. Fantner G, Hassenkam T, Kindt J, Weaver J, Birkedal H, Pechenik L, Cutroni J, Cidade G, Stucky G, Morse D, Hansma P. Nat. Mater. 2005; 4:612–616. [PubMed: 16025123]

14. Gebauer D, Colfen H. Nano Today. 2011; 6:564–584.

15. Mahamid J, Aichmayer B, Shimoni E, Ziblat R, Li C, Siegel S, Paris O, Fratzl P, Weiner S, Addadi L. Proc. Natl. Acad. Sci. U.S.A. 2010; 107:6316–6321. [PubMed: 20308589]

16. Colfen H. Nat. Mater. 2010; 9:960–961. [PubMed: 21102512]

17. Nudelman F, Pieterse K, George A, Bomans PHH, Friedrich H, Brylka LJ, Hilbers PAJ, de With G, Sommerdijk NAJM. Nat. Mater. 2010; 9:1004–1009. [PubMed: 20972429]

18. Liu P, Song J. Biomaterials. 2013; 34:2442–2454. [PubMed: 23332320]

19. Ishihara K, Nomura H, Mihara T, Kurita K, Iwasaki Y, Nakabayashi N. J. Biomed. Mater. Res. 1998; 39:323–330. [PubMed: 9457564]

20. Yuan YL, Zhang J, Ai F, Yuan J, Zhou J, Shen J, Lin SC. Colloid. Surface. B. 2003; 29:247–256.

21. Yuan JA, Bian RB, Ling T, Jian S, Lin SC. Colloid. Surface. B. 2004; 36:27–33.

22. Yan H, Zhu HM, Shen J. Sci. China Ser. B. 2007; 50:660–664.

23. Liu PS, Chen Q, Liu X, Yuan B, Wu SS, Shen J, Lin SC. Biomacromolecules. 2009; 10:2809–2816. [PubMed: 19743844]

24. Jiang S, Cao Z. Adv. Mater. 2010; 22:920–952. [PubMed: 20217815]

25. Chen SF, Li LY, Zhao C, Zheng J. Polymer. 2010; 51:5283–5293.

26. Banerjee I, Pangule RC, Kane RS. Adv. Mater. 2011; 23:690–718. [PubMed: 20886559]

27. Bose S, Roy M, Bandyopadhyay A. Trends Biotechnol. 2012; 30:546–554. [PubMed: 22939815]

28. Rezwan K, Chen QZ, Blaker JJ, Boccaccini AR. Biomaterials. 2006; 27:3413–3431. [PubMed: 16504284]

29. LeGeros RZ. Clin. Orthop. Relat. R. 2002:81–98.

30. Kutikov A, Song J. Acta Biomaterialia. 2013; 9:8354–8364. [PubMed: 23791675]

31. Xu JW, Li XN, Lian JB, Ayers DC, Song J. J. Orthop. Res. 2009; 27:1306–1311. [PubMed: 19350632]

32. Bae SE, Choi J, Joung YK, Park K, Han DK. J. Control. Release. 2012; 160:676–684. [PubMed: 22543042]

33. Bose S, Tarafder S. Acta. Biomater. 2012; 8:1401–1421. [PubMed: 22127225]

34. Liu PS, Smits J, Ayers DC, Song J. Acta. Biomater. 2011; 7:3488–3495. [PubMed: 21651998]

35. Filion TM, Li XN, Mason-Savas A, Kreider JM, Goldstein SA, Ayers DC, Song J. Tissue Eng. Pt. A. 2011; 17:503–511.

36. Zhang Z, Chao T, Chen SF, Jiang SY. Langmuir. 2006; 22:10072–10077. [PubMed: 17107002]

37. Song J, Saiz E, Bertozzi CR. J. Am. Chem. Soc. 2003; 125:1236–1243. [PubMed: 12553825]

38. Hoffman AS. Adv. Drug Deliver. Rev. 2002; 54:3–12.

39. Tas AC. J. Am. Ceram. Soc. 2001; 84:295–300.

40. Liu P, Domingue E, Ayers DC, Song J. ACS Appl. Mater. Inter. 2014; 6:7141–7152.

41. Katagiri T, Yamaguchi A, Komaki M, Abe E, Takahashi N, Ikeda T, Rosen V, Wozney JM, Fujisawasehara A, Suda T. J. Cell Biol. 1994; 127:1755–1766. [PubMed: 7798324]

42. Song J, Malathong V, Bertozzi CR. J. Am. Chem. Soc. 2005; 127:3366–3372. [PubMed: 15755154]

43. Ripin, DH.; Evans, DA. 2005. http://evans.harvard.edu/pdf/evans_pKa_table.pdf,

44. Reichmuth DS, Kirby BJ. J. Chromatogr. A. 2003; 1013:93–101. [PubMed: 14604111]

45. Kumler WD, Eiler JJ. J. Am. Chem. Soc. 1943; 65:2355–2361.

46. Liu PS, Skelly JD, Song J. Acta Biomater. 2014

47. Matsumoto T, Okazaki M, Inoue M, Yamaguchi S, Kusunose T, Toyonaga T, Hamada Y, Takahashi J. Biomaterials. 2004; 25:3807–3812. [PubMed: 15020156]

48. Kim SS, Gwak SJ, Kim BS. J. Biomed. Mater. Res. A. 2008; 87A:245–253. [PubMed: 18181112]

49. Yang HS, La WG, Bhang SH, Lee TJ, Lee M, Kim BS. Tissue Eng. Pt. A. 2011; 17:2153–2164.

50. Liu Y, Lu Y, Tian XZ, Cui G, Zhao YM, Yang Q, Yu SL, Xing GS, Zhang BX. Biomaterials. 2009; 30:6276–6285. [PubMed: 19683811]

51. Hanseler P, Ehrbar M, Kruse A, Fischer E, Schibli R, Ghayor C, Weber FE. J. Biomed. Mater. Res. A. 2014

52. Hu H, Wang XB, Xu SL, Yang WT, Xu FJ, Shen J, Mao C. J. Mater. Chem. 2012; 22:15362–15369.

53. Lin WF, Zhang H, Wu J, Wang Z, Sun HT, Yuan J, Chen SF. J. Mater. Chem. B. 2013; 1:2482–2488.

54. Yin HY, Akasaki T, Sun TL, Nakajima T, Kurokawa T, Nonoyama T, Taira T, Saruwatari Y, Gong JP. J. Mater. Chem. B. 2013; 1:3685–3693.

55. Ladd J, Zhang Z, Chen S, Hower JC, Jiang S. Biomacromolecules. 2008; 9:1357–1361. [PubMed: 18376858]

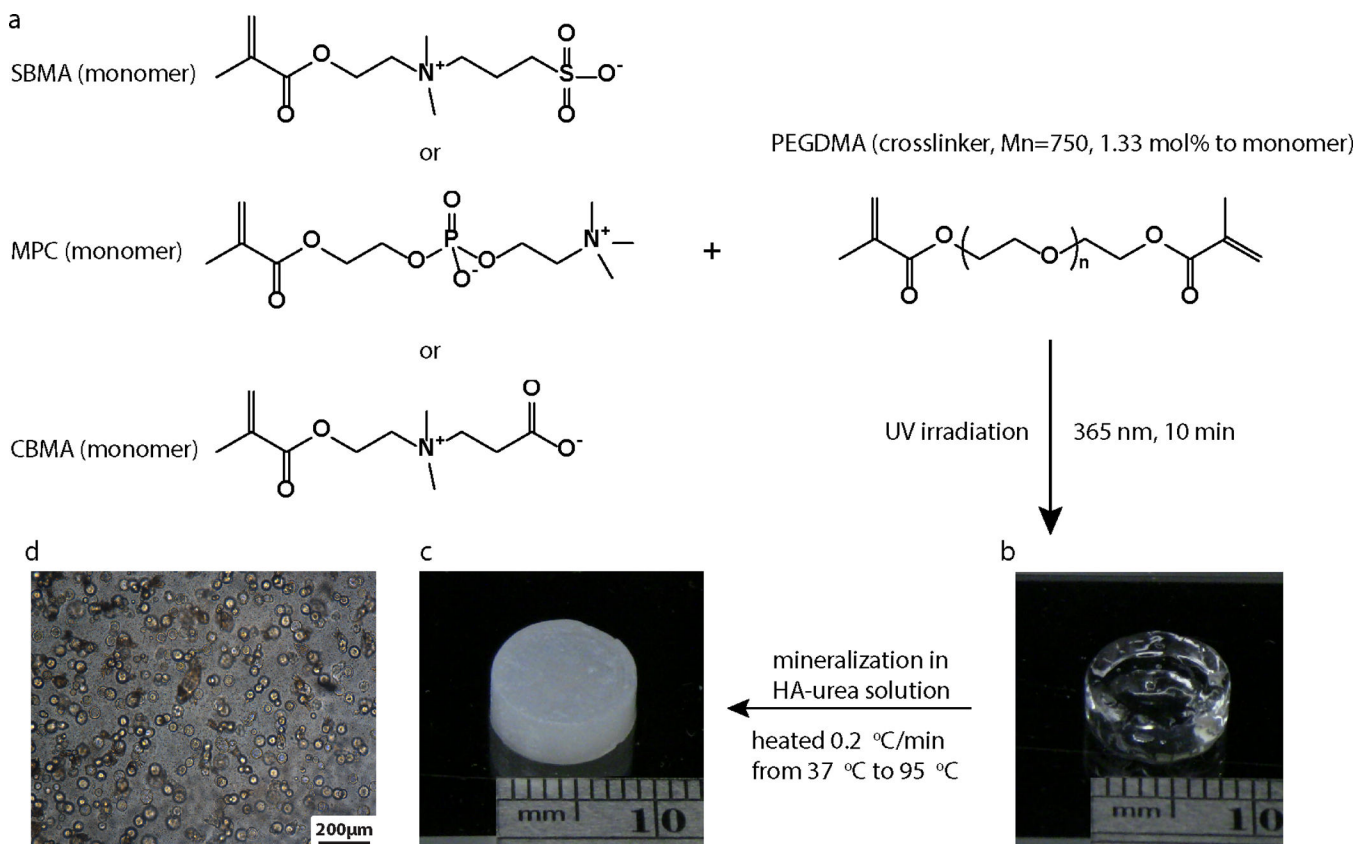56. Li Q, Bi QY, Zhou B, Wang XL. Appl. Surf. Sci. 2012; 258:4707–4717.

Figure 1.
Preparation and mineralization of the zwitterionic PSBMA, PMPC, and PCBMA hydrogels.
(a) Chemical structures of the three zwitterionic monomers and the schematics of their
photo-crosslinking. (b) A representative image of the photo-crosslinked zwitterionic
hydrogel. (c) A representative image of a mineralized zwitterionic hydrogel. The HA-
mineralization was mediated by the gradual pH increases resulting from the thermal
decomposition of urea. (d) A representative optical micrograph of the mineral nodules
formed within the zwitterionic hydrogel.
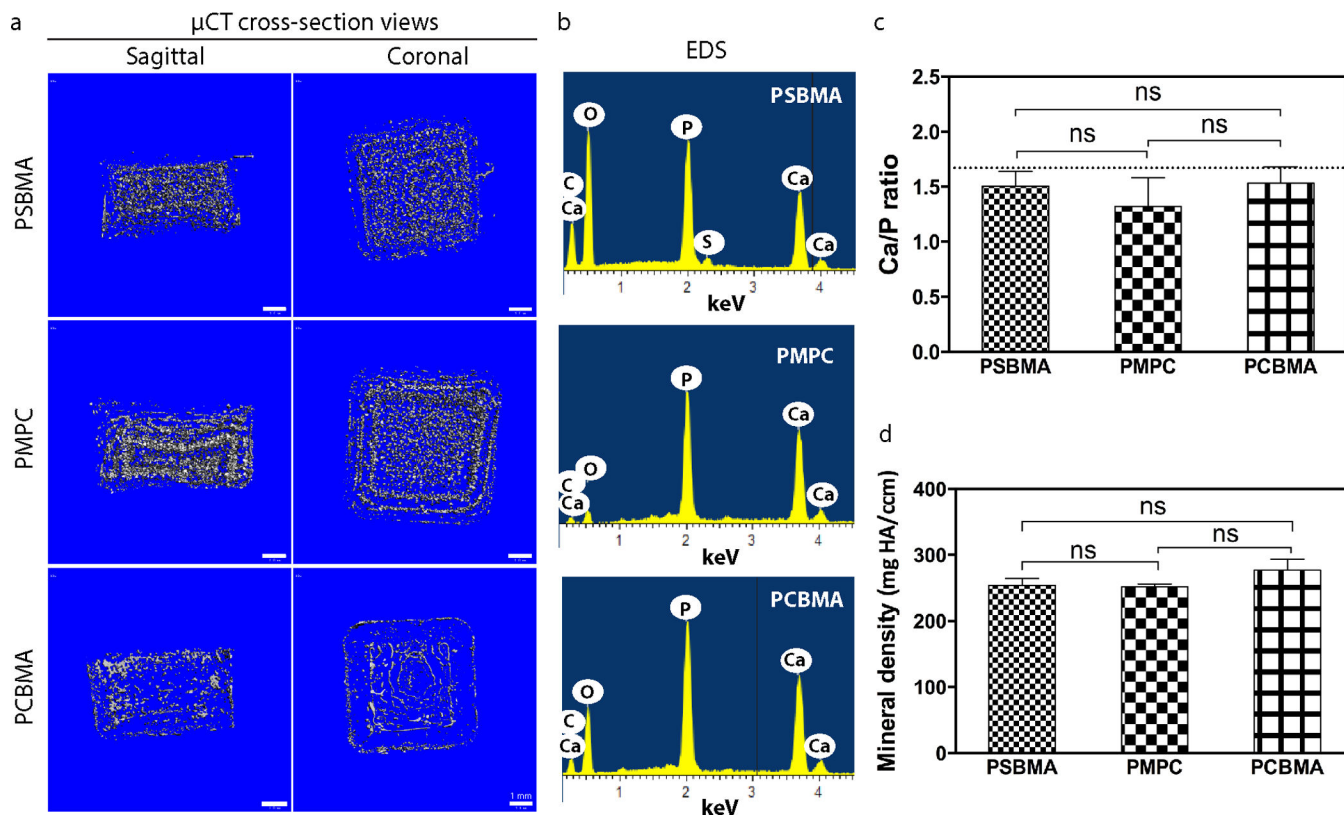
Figure 2.
Mineralization outcomes of zwitterionic PSBMA, PMPC, and PCBMA hydrogels. (a) Cross-section views of the reconstructed μ-CT images of the mineralized zwitterionic hydrogels. (b) Representative EDS spectra of the mineralized hydrogel specimens. (c) Ca/P ratio of the mineral nodules within the respective zwitterionic composites as determined by EDS. The dash line indicates the theoretical Ca/P ratio of HA (1.67). (d) Mineral density of the mineralized zwitterionic hydrogels as determined by μ-CT.
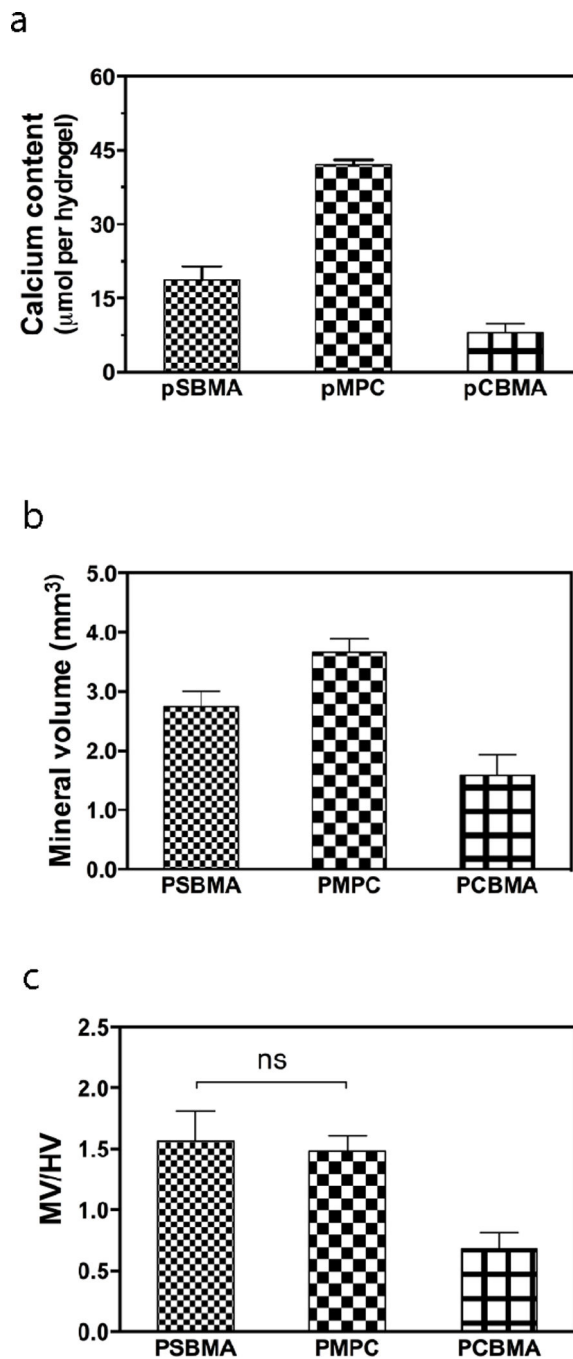
Figure 3.
Quantitative characterizations of the mineralization outcomes of zwitterionic PSBMA, PMPC, and PCBMA hydrogels. (a) Calcium content of the mineralized hydrogels determined by quantitation of the Ca^{2+} released upon acid-treatment. (b) Mineral volume as determined by μ-CT. (c) Mineral volume/hydrogel volume (MV/HV) as determined by μ-CT. All differences are significant ($p < 0.05$; One-way ANOVA multiple comparison) unless denoted as ns (not significant).
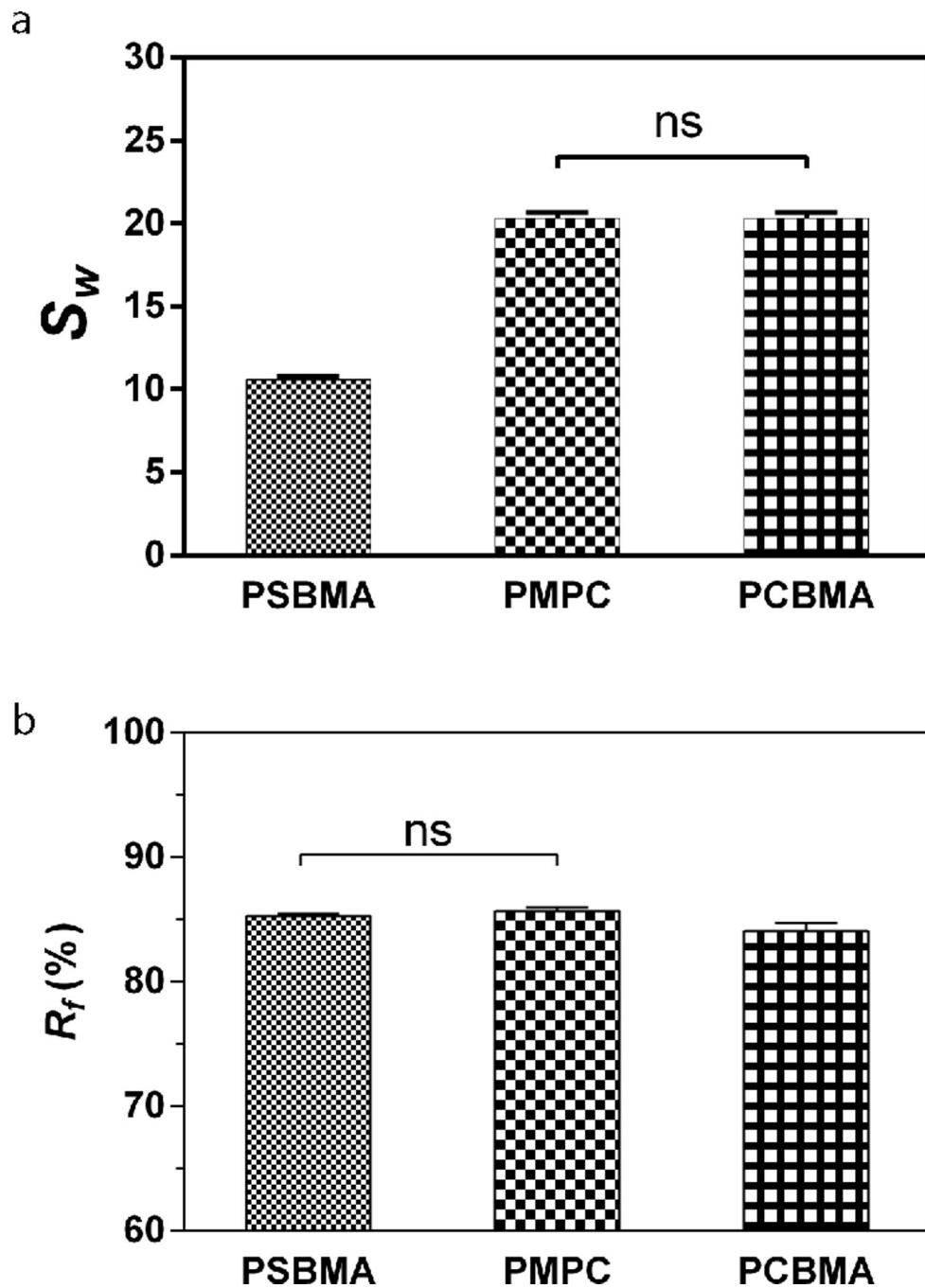
a

b

Figure 4.
Swelling ratio (a) and free water fraction (b) of the zwitterionic PSBMA, PMPC, and
PCBMA hydrogels equilibrated in PBS (pH=7.4). All differences are significant ($p < 0.05$;
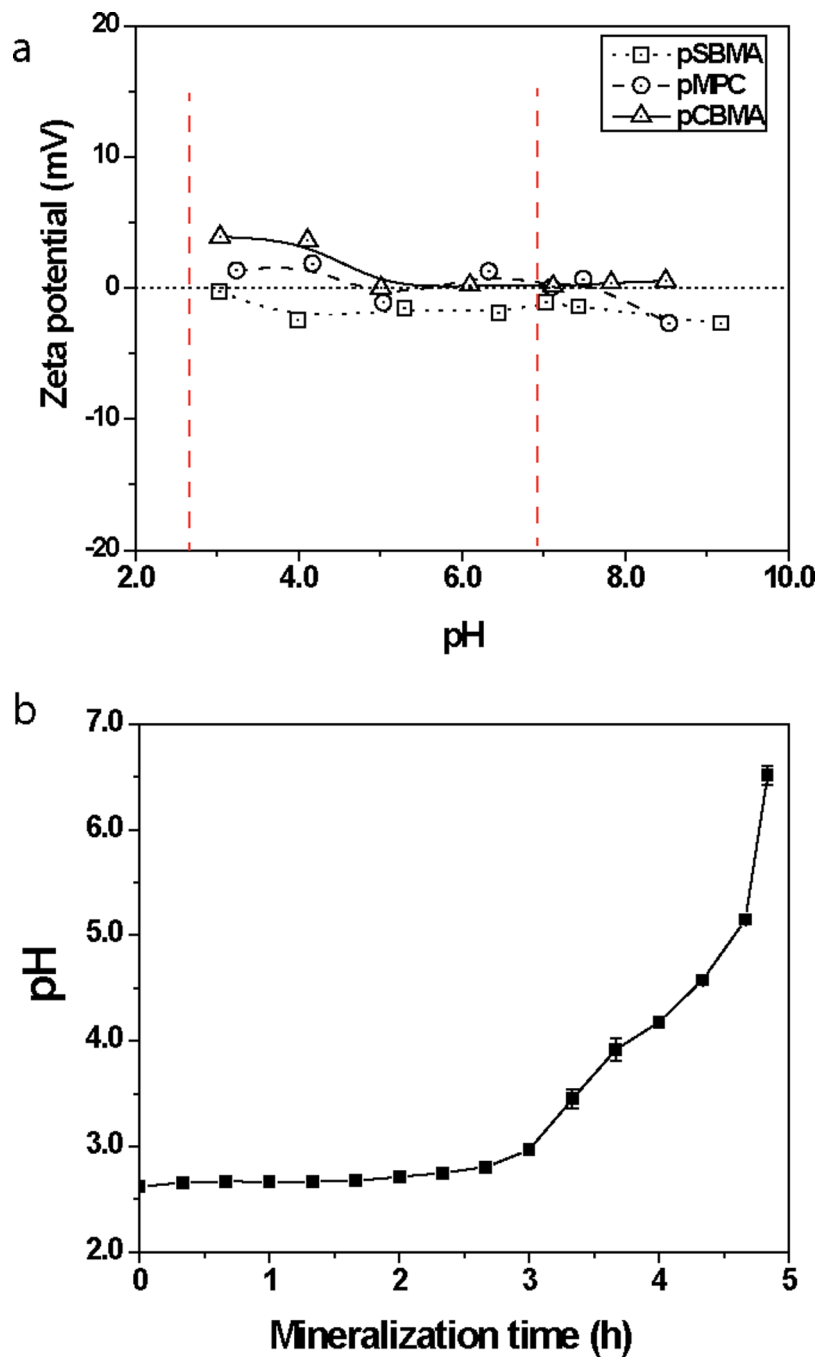One-way ANOVA multiple comparison) unless denoted as ns (not significant).

Figure 5.
Zeta potential of the linear zwitterionic PSBMA, PMPC, and PCBMA polymers as a
function of pH (a) and the temporal pH changes during the mineralization process (b). Red
dash lines in (a) indicate the pH range of the in vitro mineralization process.
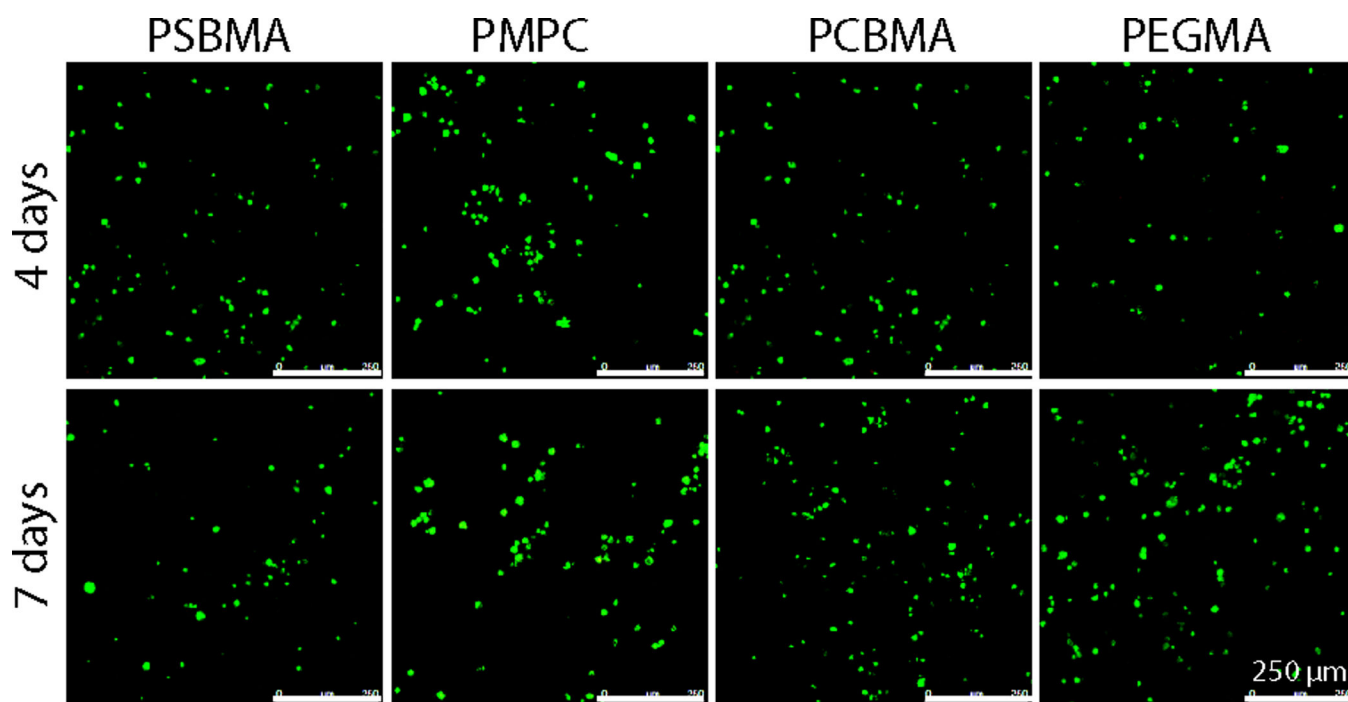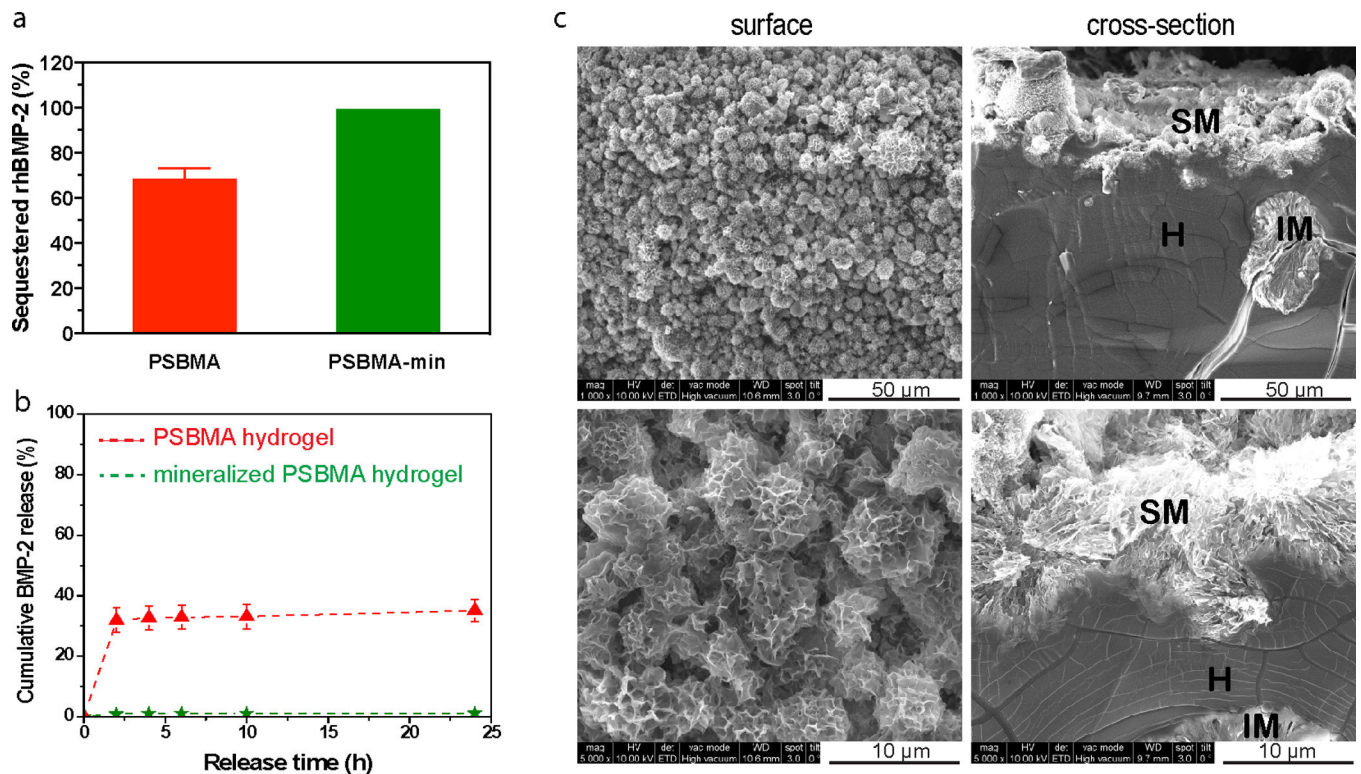
Figure 6.
Confocal Z-stack (80 μm) images of live (green)/dead (red) rMSCs encapsulated in the zwitterionic PSBMA, PMPC, and PCBMA vs. PEGMA hydrogels after up 4- or 7-day culture.
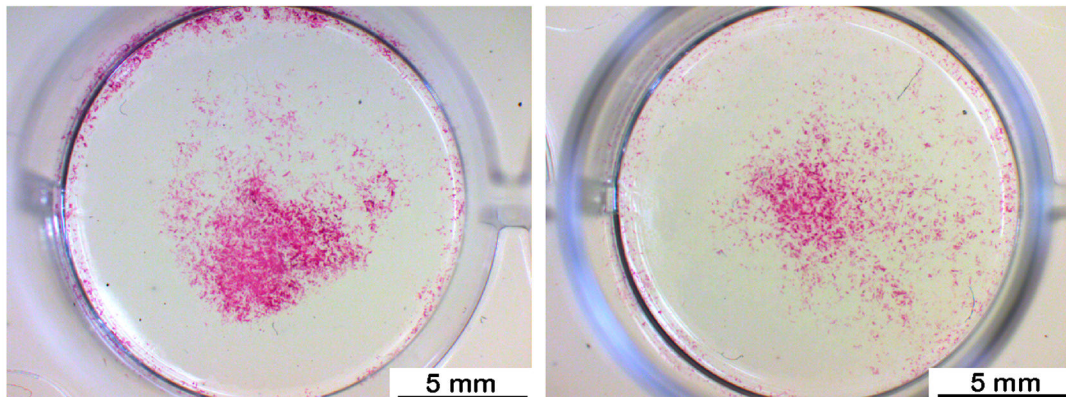
Figure 7. fdjhngfdkfdk
Retention and sustained release of rhBMP-2 from mineralized PSBMA hydrogel. (a) Sequestering efficiency of the rhBMP-2 by PSBMA hydrogels and mineralized PSBMA after 2-h incubation in PBS. 300-ng rhBMP-2 was loaded to each specimen. (b) rhBMP-2 release profiles from PSBMA and mineralized PSBMA hydrogels. (c) SEM images micrographs (surface & cross-section views) of the mineralized PSBMA hydrogel at different magnifications. H = hydrogel, SM = surface mineral domains, and IM = interior mineral domains. (d) Robust osteogenic trans-differentiation of C2C12 cells induced by the rhBMP-2 released from mineralized PSBMA hydrogel from day 7 to day 9 (pre-incubated in

PBS for 6 days prior to placement in C2C12 culture). C2C12 culture directly supplemented with 300-ng rhBMP-2 without any hydrogel carrier served as a positive control.
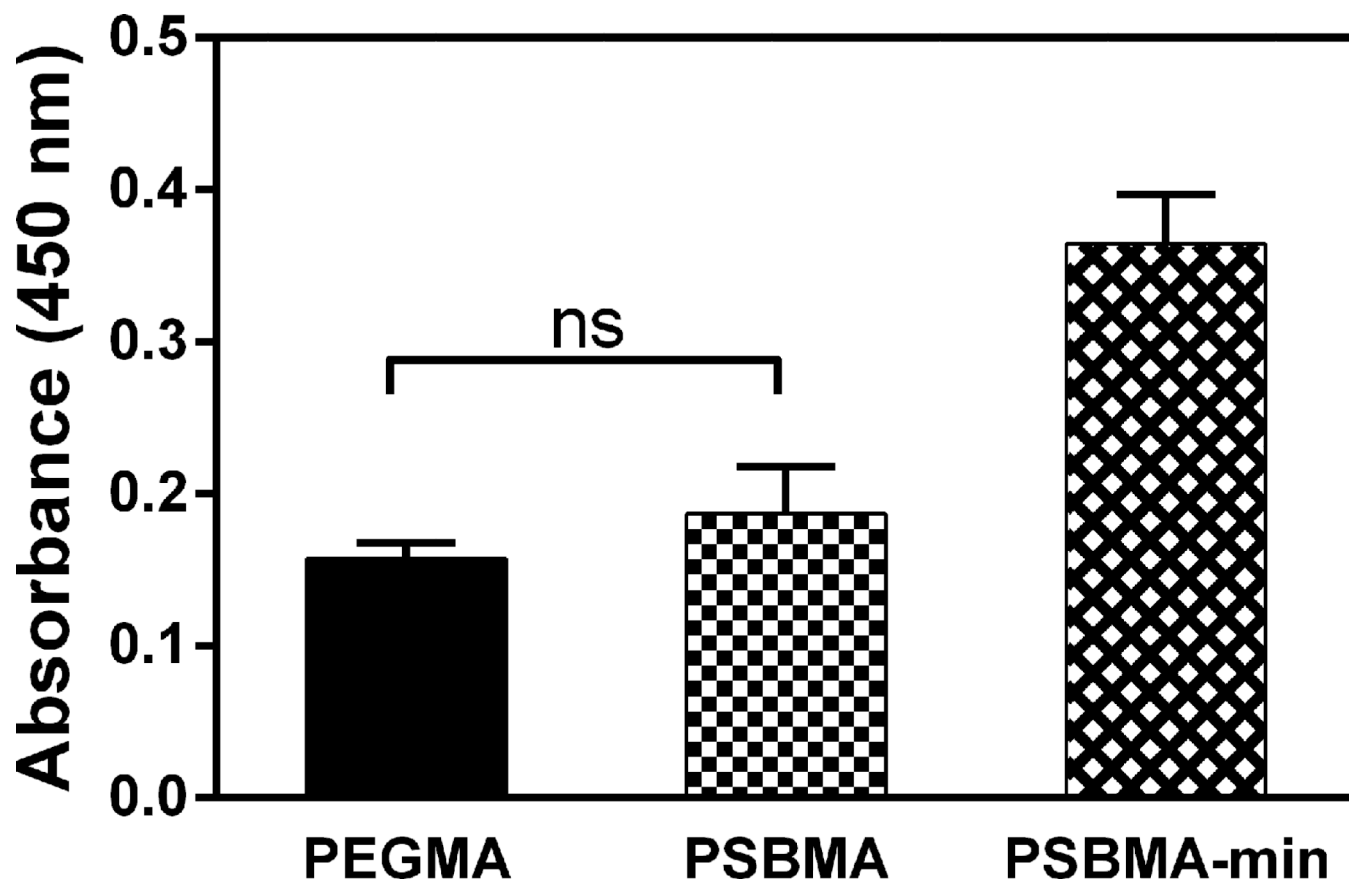
Figure 8.
rMSC attachment on PSBMA, mineralized PSBMA and PEGMA hydrogels as determined by CCK-8 viability assay 24 h after initial cell seeding. All differences are significant (p < 0.05; One-way ANOVA multiple comparison) unless denoted as ns (not significant).

Table 1

Molecular weight and molecular weight distribution (PDI) of linear zwitterionic polymers prepared by atom transfer radical polymerization.

polymer	M_n (g/mol)	M_w (g/mol)	PDI (M_w/M_n)
PSBMA	12424	13596	1.09
PMPC	13476	15328	1.14
PCBMA	15700	21866	1.39